Spectrum Investment under Uncertainty: A Behavioral Economics Perspective

Junlin Yu, *Student Member, IEEE*, Man Hon Cheung, and Jianwei Huang, *Fellow, IEEE*

Abstract—In this paper, we study a virtual wireless operator's spectrum investment problem under spectrum supply uncertainty. To obtain enough spectrum resources to meet its customer demands, the virtual operator can either sense for the temporarily unused spectrum in a licensed band, or lease spectrum from a spectrum owner. Sensing is usually cheaper than leasing, but the amount of available spectrum obtained by sensing is uncertain due to the primary users' activities in the licensed band. Previous studies on spectrum investment problems mainly considered the expected profit maximization problem of a risk-neutral operator based on the expected utility theory (EUT). In reality, however, an operator's decision is influenced by not only the consideration of expected profit maximization, but also the level of its risk preference. To capture this tradeoff between these two considerations, we analyze the operator's optimal decision problem using the prospect theory from behavioral economics, which includes EUT as a special case. The sensing and leasing optimal problem under prospect theory is non-convex and challenging to solve. Nevertheless, by exploiting the unimodal structure of the problem, we are able to compute the unique global optimal solution. We show that comparing to an EUT operator, both the risk-averse and risk-seeking operator achieve a smaller expected profit. On the other hand, a risk-averse operator can guarantee a larger minimum possible profit, while a risk-seeking operator can achieve a larger maximum possible profit. Furthermore, the tradeoff between the expected profit and the minimum possible profit for a risk-averse operator is better when the sensing cost increases, while the tradeoff between the expected profit and the maximum possible profit for a risk-seeking operator is better when the sensing cost decreases.

Index Terms—Prospect theory, expected utility theory, spectrum trading, spectrum sensing.

I. INTRODUCTION

A. Background and Motivation

THE business model of *virtual operator*[1] has achieved significant success worldwide in recent years [2]. According to a recent market report published by Transparency Market Research, the global virtual operator market is expected to expand at an annual rate of 7.4% and reach a value of US$ 75.25 billions by 2023 [3]. As a virtual operator (e.g., Consumer Cellular in the US [4]) does not own any licensed spectrum, it needs to acquire spectrum from a *spectrum owner* (e.g., AT&T) in order to provide services to its customers. As virtual operators often rely on leased network infrastructure instead of building and maintaining their own infrastructure, their investment and operational costs are usually lower than the spectrum owners. Such an advantage often enables them to provide cheaper and more flexible data plans to their customers, hence reaching niche markets that are underserved by the spectrum owners [5].

Motivated by the recent development of cognitive radio technology and dynamic spectrum sharing, a virtual operator can acquire spectrum in two different ways: spectrum sensing and spectrum leasing. With *spectrum sensing* [6], [7], a virtual operator detects the temporarily unused spectrum in a licensed band, and uses it to provide services to its customers as long as such operator does not cause any harmful interferences to the primary (licensed) customers of the spectrum owner. With *spectrum leasing* [8], [9], a spectrum owner explicitly allows the virtual operator to operate over a given licensed band during a given period of time with a leasing fee. In this paper, we will consider a hybrid spectrum investment scheme involving both approaches.

The key feature of the problem is the uncertainty of spectrum acquisition through spectrum sensing, as the virtual operator does not know the activity levels of the primary customers beforehand. When facing uncertainty, most prior studies of spectrum investment applied the *expected utility theory* (EUT) to compute the operator's optimal decisions (e.g., [10]–[13]). In these models, a (virtual) operator optimizes the decisions to maximize its expected profit. Such an EUT model, however, does not fully capture the rather complicated decision process obtained in our daily life, and hence may have a poor predication power [14]. Alternatively, the Nobel-prize-winning *prospect theory* (PT) (e.g., [14]–[16]), which establishes a more general model than the EUT, provides a psychologically more accurate description of the decision-making under uncertainty. PT[2] incorporates three main factors in the modeling: (1) *Impact of reference point*: A decision maker evaluates an option based on the potential gains or

J. Yu, M. H. Cheung, and J. Huang are with the Department of Information Engineering, the Chinese University of Hong Kong, Hong Kong, China; Emails: {yj112, mhcheung, jwhuang}@ie.cuhk.edu.hk.

[1]Here we focus on a "virtual operator" in the wireless industry, which is also referred to as the "mobile virtual network operator (MVNO)" in the literature.

[2]To better understand PT, consider the following two lottery settings. Lottery A1: 50% to win $200, and 50% to win $0; Lottery A2: 100% to win $100. Experimental results [14] showed that most people prefer Lottery A2 to A1. The result reflects that people are risk averse, which we will discuss in more details later in this section. Next we further consider another two lottery settings. Lottery B1: 1% to win $99, and 99% to loss $1; Lottery B2: 100% to win $0. Experimental results [14] showed that most people prefer Lottery B1 to B2. The result reflects that people will have a subjective probability distortion of small probability events, which we will also introduce later in this section.

losses with respect to a reference point, and the choice of the reference point significantly affects the valuation. (2) The *s-shaped asymmetrical value function*: A decision maker often experiences a diminishing marginal utility when evaluating a gain, and a diminishing marginal disutility when evaluating a loss. Furthermore, it often prefers avoiding losses than achieving gains. As a result, the value function is s-shaped and asymmetrical: concave in the gain regime, convex in the loss regime, and steeper for losses than for gains (see Fig. 2(a) in Section III-D for a concrete example). (3) *Probability distortion*: A decision maker tends to overreact to small probability events, but underreact to medium and large probability events (see Fig. 2(b) in Section III-D for a concrete example). This characteristic is useful in explaining behaviors related to lottery and insurance [14], where people usually purchase lottery and insurance at prices higher than the expected returns. As PT fits better into the reality than EUT based on many empirical studies, researchers and practitioners have applied PT in many areas, such as understanding the behavior of investment agents in finance [17] and the effort and wage levels of workers and firms in labor markets[3] [20]. However, there isn't any existing work of using PT to understand the spectrum investment behaviors in today's wireless market.

B. Key Results and Contributions

In this paper, we study the spectrum sensing and leasing decisions of a virtual operator under sensing *uncertainty*, and formulate it as a two-stage sequential optimization problem. In Stage I, the virtual operator determines the optimal amount of licensed spectrum to *sense*. Due to the stochastic nature of the primary licensed customers' traffic, the amount of available spectrum obtained through sensing is a random variable. If the spectrum obtained through sensing is not sufficient to satisfy its customers' demand, the virtual operator will *lease* some additional spectrum from the spectrum owner in Stage II.

Under this sensing *uncertainty*, we can model the decision making of a risk-neutral operator, who aims to maximize its expected profit by EUT. However, in reality, a decision maker is rarely risk-neutral. Besides aiming to achieve a high expected profit, it is often affected by its own risk preference. To be more specific, a risk-seeking decision maker is aggressive and wants to achieve a high profit even with a high risk, while a risk-averse decision maker is conservative and wants to guarantee a satisfactory level of minimum possible profit. In order to capture this tradeoff between the expected profit and risk preference, we apply the PT to study the optimal sensing and leasing decisions. It leads to a *non-convex* optimization problem, which is very challenging to solve. Nevertheless, by exploiting the unimodal structure of the problem, we can obtain the *global optimal* solution analytically.

Our key contributions are summarized as follows:

---

[3]We note that prospect theory is not a theory only about "irrational behaviors". Instead, it is about how decision makers decide the tradeoff between the maximum/minimum possible profit and the expected profit (in our context), which applies to professionals as well. In fact, there have been various studies (e.g., [18], [19]) that focus on the professionals' decisions problems based on prospect theory in areas such as finance and politics.

- *Behavioral economics modeling of virtual operator's investment decision under uncertainty*: We model a virtual operator's investment decisions under sensing uncertainty using PT, which captures the tradeoff between the expected profit maximization and risk preference. We characterize the feature of a risk-averse operator (who is most concerned of potential losses) and a risk-seeking operator (who is most concerned of potential gains).
- *Characterization of the unique optimal solution of the non-convex decision problem*: Despite the non-convexity of the spectrum sensing problem, we characterize the uniqueness of the optimal solution and compute it numerically. We further evaluate how different behavioral characteristics (i.e., reference point, probability distortion, and s-shaped valuation) affect this optimal solution.
- *Engineering insights based on comparison between EUT and PT*: We show that a risk-averse operator can achieve a better tradeoff between the expected profit and minimum possible profit in the high sensing cost scenario than the low sensing cost scenario. The result for the risk-seeking operator is exactly the opposite.

Next we will review the literature in Section II. In Section III, we introduce the spectrum investment model and formulate the sequential optimization problem. In Section IV, we compute the global optimal solution of the non-convex optimization problem, and discuss various engineering insights derived from such a solution. In Section V, we illustrate the impact of probability distortion and reference point by considering the special case of binary sensing outcomes. In Section VI, we provide simulation results to evaluate the sensitivity of the optimal decision with respect to several model parameters. We conclude the paper in Section VII.

II. LITERATURE REVIEW

A. Expected Profit Maximization in Spectrum Investment Using Expected Utility Theory

Spectrum investment problem under uncertainty has been studied extensively through expected profit maximization using EUT (e.g., [10]–[13]). Kasbekar and Sarkar in [10] considered a spectrum auction problem under the uncertainty of the number of secondary customers. Gao *et al.* in [11] studied the spectrum contract between a primary spectrum owner and the secondary customers considering the uncertainty of the customer types. In [12], Jin *et al.* presented an insurance-based spectrum trading problem between a primary spectrum owner and the secondary customers, where the uncertainty also comes from the types of the customers. Duan *et al.* in [13] considered the spectrum investment of a virtual operator under the spectrum sensing uncertainty. In all the above studies based on EUT, a decision maker aims to maximize the weighted average of its utilities under different outcomes, which does not fully capture the realistic human decision behaviors examined in several well known psychological studies in the past few decades [14]–[16]. Thus, in this paper we apply the more general PT, which takes into account both the expected payoff and risk preference in the human decision making.

B. Resource Allocation in Communication Networks and Smart Grids Using Prospect Theory

The study of resource allocation in communication networks and smart grids based on PT only emerged recently. The first paper is due to Li *et al.* in [21], which compared the equilibrium strategies of a two-user random access game under EUT and PT. Yang *et al.* in [22] considered the impact of end-user decision-making on wireless resource pricing, when there is an uncertainty in the quality of service (QoS) guarantees relying on PT. Several other recent studies applied PT to study the decision making in smart grid systems. In [23], Wang *et al.* formulated a non-cooperative game among consumers in an energy exchange system. They applied PT to explicitly account for the users' subjective perceptions of their expected utilities. Xiao *et al.* in [24] studied the static energy exchange game among microgrids that are connected to a backup power plant. They analyzed the Nash equilibria under various scenarios based on PT, and evaluated the impact of user's objective weight on the equilibrium of the game. To reflect the fact that realistic decision making is different from expected profit maximization, the studies in [21]–[24] considered a linear value function with the probability distortion. However, to model the impact of risk preference on a decision maker, using only a linear value function is not comprehensive enough. In fact, based on the psychological studies in [14]–[16], the three characteristics of PT (i.e., reference point, s-shaped value function, and probability distortion) together determine the risk preference of a decision maker. Our paper is the first one that considers all three characteristics of PT for a more accurate and comprehensive understanding of the optimal decision problem.

III. SYSTEM MODEL

A. Spectrum Sensing and Leasing Tradeoff

We consider a cognitive radio network with a spectrum owner and a virtual operator. From the empirical data in [25], [26], it is possible for the spectrum owner to estimate the spectrum utilization at a particular location accurately based on past measurements. In this paper, we assume that such estimations are accurate, so that the spectrum owner can divide its licensed spectrum into the *primary band* and *secondary band* according to the spectrum utilization. The spectrum owner uses the primary band to serve its primary customers (PCs), while reserves the secondary band to meet the potential leasing requests from the virtual operator. For the virtual operator, it can either try to sense the idle spectrum in the primary band (as PCs' activities are stochastic during the time period of interest), or lease the spectrum from the secondary band.

As a more concrete (hypothetical) example, we consider the spectrum trading between Consumer Cellular and AT&T (shown in Fig. 1). AT&T is a spectrum owner, who provides wireless services to its PCs. However, it cannot fully utilize its spectrum in some rural areas, so it will divide its spectrum into the primary band (channel 1-8) and secondary band (channel 9-16) at those under-utilized locations. Consumer Cellular wants to provide spectrum services to its own customers, but
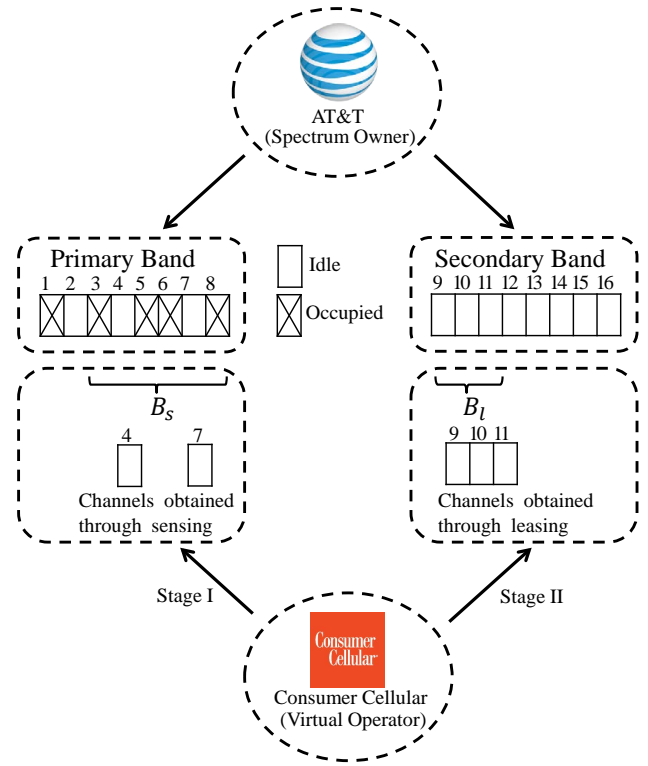

Fig. 1. An Example of Consumer Cellular and AT&T.

it does not own any spectrum. As a result, Consumer Cellular senses for spectrum holes (not used by the PCs) in the primary band (channel 3-8) without explicit payment to AT&T, and can also choose to lease spectrum in the secondary band (channel 9-11) with explicit payment to AT&T.

From the virtual operator's point of view, sensing is often a cheaper way to obtain spectrum than leasing, because the energy and time overhead involved in sensing is often much lower than the explicit cost of spectrum leasing [13]. However, the available amount of spectrum obtained through sensing is uncertain due to the spectrum owner PCs' stochastic activities over time. We would like to understand the virtual operator's optimal spectrum investment decisions in every time slot that strike the best tradeoff between the cost and the risk[4].

B. Two-Stage Decision Model

We formulate the virtual operator's spectrum investment problem as a two-stage sequential optimization problem in each time slot.

In Stage I (i.e., the sensing stage), the virtual operator determines its sensing decision B_s (measured in Hz). For simplicity, we assume a linear sensing cost c_s per unit of sensed bandwidth, which represents the time and energy overhead for sensing [27]. Due to the stochastic nature of PCs' traffic, only a fraction $\alpha \in [0, 1]$ of the sensed spectrum is temporarily available and can be utilized by the virtual operator's own customers. Hence, the virtual operator obtains a bandwidth of $B_s\alpha$[5] at the end of the stage. In other words, a

---

[4]We choose the length of time slot such that the primary customers' activities remain unchanged within a time slot [13].

[5]For simplicity, we assume perfect sensing in this paper. For imperfect sensing [28], it involves an additional level of uncertainty, which is challenging to consider due to the framing effect [14] in behavioral economics.

large α corresponds to a *high sensing realization*, and a small α corresponds to a *low sensing realization*. As an example in Fig. 1, Consumer Cellular senses six channels in Stage I (i.e., channel 3-8), and only channels 4 and 7 are available. Hence, $\alpha = 1/3$ in this case. We assume that the virtual operator knows the distribution of α through historical sensing results[6]. Notice that in the sensing stage, the virtual operator has uncertainty of sensing realization, and its optimal decision will be influenced by balancing the expected profit and its risk preference on the sensing uncertainty. We will discuss the PT modeling on this aspect in more details in Section III-D.

In Stage II (i.e., the leasing stage), the virtual operator determines the leasing decision B_l (measured in Hz) after knowing the available amount of spectrum through sensing, $B_s\alpha$. We consider a linear leasing cost c_l, which is determined through negotiation between the virtual operator and spectrum owner and is considered to be a fixed parameter in our model. As an example in Fig. 1, after Consumer Cellular acquires two channels from sensing (i.e., channels 4 and 7), it further leases three more channels in Stage II (i.e., channel 9-11). As there is no uncertainty involved in Stage II, there is no difference between EUT and PT modeling in terms of results[7].

C. Virtual Operator's Profit

When serving its customers, the virtual operator can obtain a revenue of π per unit of sold spectrum. We assume that the price π is exogenously given and cannot be changed by the virtual operator, due to the intensive market competition [35]. Under a fixed usage-based price π, we assume that the virtual operator's secondary customers' maximum spectrum (bandwidth) demand is D[8]. However, the demand may not be fully satisfied if the virtual operator does not have enough spectrum obtained through sensing and leasing discussed before. Hence, the profit of the virtual operator is

$$R(B_s, B_l, \alpha) = \pi \min\{D, B_l + B_s\alpha\} - (B_s c_s + B_l c_l), \quad (1)$$

where the revenue (first term on the right hand side) depends on the minimum of the demand D and the spectrum supply $B_l + B_s\alpha$, and the cost (second term on the right hand side) depends on both the sensing decision B_s and leasing decision B_l. As α is a random variable before making the sensing decision B_s, we will incorporate the operator's risk preference towards such uncertainty through the modeling based on prospect theory.

D. Prospect Theory Modeling in Sensing Decision

To model the virtual operator's decision under spectrum sensing uncertainty, we consider the following three key

[6] In practice, it is difficult for the operator to obtain the exact distribution of α. However, according to [29]–[32], the operator can estimate the distribution of α through learning based on the updated historical sensing results [33], [34].

[7] In fact, as long as $\lambda = \beta = \alpha = 1$, choosing a non-zero value of R_p will just induce a constant shift of the EUT utilities, without affecting the optimal decision under EUT. The reference point affects the analysis of PT, and our analysis shows the impact of reference point in Section V-B.

[8] We do not assume any specific relationship between price π and demand D in this paper. Please refer to [35] for some further discussions along this line.
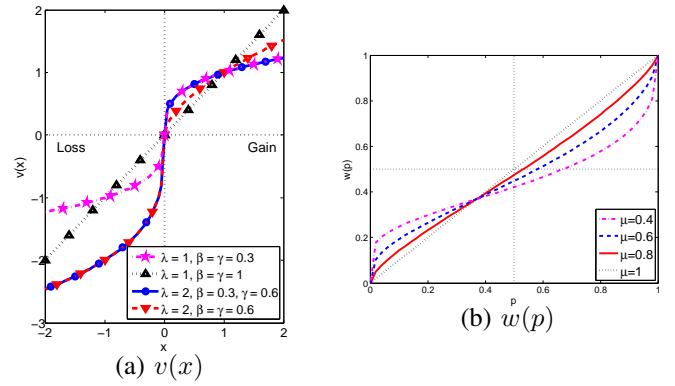

Fig. 2. The s-shaped asymmetrical value function $v(x)$ and the probability distortion function $w(p)$ in PT.

features of PT: *reference point* R_p, s-shaped *value function* $v(x)$, and *probability distortion function* $w(p)$.

First, the choice of reference point R_p will significantly affect the evaluation of profit $R(B_s, B_l, \alpha)$ in PT. More specifically, we define the net gain as

$$x = R(B_s, B_l, \alpha) - R_p. \quad (2)$$

The reference point is a benchmark to evaluate the payoff, where $x \geq 0$ means a gain, while $x < 0$ means a loss. The virtual operator will have different decision mechanisms (to be explained in the next paragraph) when dealing with a gain or a loss in PT. A higher reference point means that the operator expects a higher profit (at the benchmark), which implies the operator is more risk-seeking.

Second, as shown in Fig. 2(a), the value function $v(x)$ is concave for a positive argument (gain), and is convex for a negative argument (loss). Moreover, the impact of loss is usually larger than the gain of the same absolute value. A common choice of value function [15], [16], [36] is

$$v(x) = \begin{cases} x^\beta, & \text{if } x \geq 0, \\ -\lambda(-x)^\gamma, & \text{if } x < 0, \end{cases} \quad (3)$$

where $\lambda > 1$, $0 < \beta < 1$, and $0 < \gamma < 1$. The parameter λ is the loss penalty parameter, where a larger λ indicates that the virtual operator is more concerned of loss, and hence is more *risk-averse*. The parameters β and γ are the risk parameters, where the value function of the gain part is more concave (i.e., the virtual operator is more *risk-averse*) when β approaches zero, and the value function of the loss part is more convex (i.e., the virtual operator is more *risk-seeking*) when γ approaches zero. The impact of β and γ can be interpreted by the risk-seeking behavior in loss and risk-averse behavior in gain. As an example, a gambler will be more addicted into the gambling when it loses money, and will be less willing to continue when he wins money.

We note that EUT is a special case if we choose $\lambda = 1$ and $\gamma = \beta = 1$. The result under the case $\gamma = \beta$ has been discussed in the conference version of this work in [1], and we focus on the more complicated case of $\beta < \gamma$ in this paper[9],

[9] The analysis can be readily extended to the case of $\beta > \gamma$, although there are no additional new insights in that case. Hence we omit the discussion of $\beta > \gamma$ here.

TABLE I
KEY NOTATIONS

Symbols	Physical Meanings
B_s (decision variable)	Sensing amount
B_l (decision variable)	Leasing amount
c_s	Sensing cost per unit
c_l	Leasing cost per unit
π	Price per unit
D	Secondary users' demand
α	Sensing realization factor
β	Risk parameter for gain
γ	Risk parameter for loss
λ	Loss penalty parameter
μ	Probability distortion parameter

which models the scenario that the marginal utility in gain is diminishing faster than the marginal disutility in loss [37].

Assumption 1. *The risk parameter for gain is less than the risk parameter for loss (i.e., $\beta < \gamma$).*

Third, as shown in Fig. 2(b), the probability distortion function $w(p)$ models the fact that virtual operator overweighs a small probability event and underweighs a large probability event. A common choice of probability distortion function (e.g., [15], [16], [36]) is

$$w(p) = \exp\left(-(-\ln p)^\mu\right), \ 0 < \mu \leq 1, \quad (4)$$

where p is the *objective* probability of high sensing realization, and $w(p)$ is the virtual operator's corresponding *subjective* probability. Here the probability distortion parameter μ reveals how a virtual operator's subjective evaluation distorts the objective probability, where a smaller μ means a larger distortion.

The key notations of the virtual operator's profit maximization problem are listed in Table I. In the next section, we will study the virtual operator's optimal sensing and leasing decisions that maximize its profit[10].

IV. SOLVING THE TWO-STAGE OPTIMIZATION PROBLEM

In this section, we use backward induction [38] to solve the two-stage sequential optimization problem. In Section IV-A, we derive the operator's optimal leasing decision in Stage II. In Section IV-B, we obtain the operator's optimal sensing decision in Stage I under sensing uncertainty by the PT model[11].

A. Optimal Leasing Decision in Stage II

In Stage II, given a fixed value of sensing bandwidth B_s determined in Stage I, the operator's leasing optimization problem is

$$\max_{B_l \geq 0} \ R(B_s, B_l, \alpha) = \pi \min\{D, (B_l + B_s\alpha)\} - (B_s c_s + B_l c_l).$$
$$(5)$$

In our analysis, we make the following assumptions.

[10]We will simply use "operator" to denote "virtual operator" for the rest of the paper.

[11]It should be noted that the models under EUT and PT share the same Stage II (i.e., the leasing stage), because uncertainty only appears in Stage I (i.e., the sensing stage).

Assumption 2. *(a) The sensing cost is less than the leasing cost (i.e., $c_s < c_l$); (b) The leasing cost is less than the operators usage-based price (i.e., $c_l < \pi$).*

Both parts of Assumption 2 allow us to focus on the non-trivial case in our analysis. When $c_s \geq c_l$, we can show that the operators' optimal decision of the two-stage process is always $B_s^* = 0$ and $B_l^* = D$ for any type of risk preferences, because leasing is both cheaper and risk-free. When $c_l \geq \pi$, we can show that the operator will always choose $B_l^* = 0$ for any type of risk preferences. Hence, we can focus on Assumption 2 without loss of any generality. Under Assumption 2, we can show that the optimal leasing decision that solves Problem (5) is

$$B_l^* = \max\{D - B_s\alpha, 0\}, \quad (6)$$

which is the difference between the total demand D and the available spectrum through sensing, $B_s\alpha$. If $B_s\alpha$ exceeds D, then $B_l^* = 0$. Under (6), the operator's profit in (1) can be written as a function of B_s and α:

$$R(B_s, B_l^*, \alpha) = \pi D - B_s c_s - \max\{D - B_s\alpha, 0\}c_l. \quad (7)$$

B. Optimal Sensing Decision in Stage I

We assume that the sensing realization factor α follows a discrete distribution with I possible outcomes[12], hence has a finite number of sensing realization outcomes [28], [39]. The corresponding probability mass function is denoted as

$$p(\alpha_i) \triangleq \mathbb{P}(\alpha = \alpha_i) = p_i, \quad i \in \mathcal{I} = \{1, ..., I\}. \quad (8)$$

Without loss of generality, we assume that $\alpha_i < \alpha_j$ if $i < j$. By substituting (2), (3), (4) and (8) into (7), we obtain the *expected utility* of the operator under PT as

$$U(B_s) = \sum_{i=1}^{I} v\left[R(B_s, B_l^*, \alpha_i) - R_p\right] w(p(\alpha_i))$$
$$= \sum_{i=1}^{I} v\left[\pi D - (B_s c_s + \max\{D - B_s\alpha_i, 0\}c_l) - R_p\right] w(p(\alpha_i)).$$
$$(9)$$

The operator's spectrum sensing optimization problem in Stage I with sensing uncertainty is

$$\max_{B_s \geq 0} \ U(B_s). \quad (10)$$

1) Optimal Sensing Decision under a Risk-free Reference Point $R_p = D(\pi - c_l)$: Problem (10) is a *non-convex* optimization problem, because it involves the s-shaped value function in (3). Hence, it is challenging to analytically characterize the closed-form optimal solution. However, we can show that there exists a *unique* global optimal solution by exploiting the special *unimodal* structure of the problem.

In problem (10), a common choice of reference point is the risk-free profit[13]. For example, in finance, investors naturally

[12]Since the spectrum is usually divided into a finite number of channels in practical systems, it is reasonable to consider a discrete distribution of α. Mathematically, when we choose the number of possible realizations I to be large, then the discrete distribution can well approximate a continuous distribution.

[13] A complete analysis for an arbitrary reference point is challenging because of the non-convexity in Problem (10). In Section V, we will further look into the impact of reference point in a simplified model with binary sensing results.

TABLE II
OPTIMAL SENSING AND LEASING DECISION UNDER PT

Condition	Optimal Sensing Decision B_s^*	Optimal Leasing Decision B_l^*
$D \leq M_{\hat{i}+1}$	$B_s^* = \frac{D}{\alpha_{\hat{i}+1}}$	$B_l^* = \max\{0, D - \frac{D\alpha}{\alpha_{\hat{i}+1}}\}$
$M_j < D < H_j$ for $j = \hat{i}+1, ..., I-1$	$B_s^* = g_j^{-1}(0)$	$B_l^* = \max\{0, D - \alpha g_j^{-1}(0)\}$
$H_j \leq D < M_{j+1}$ for $j = \hat{i}+1, ..., I-1$	$B_s^* = \frac{D}{\alpha_{j+1}}$	$B_l^* = \max\{0, D - \frac{D\alpha}{\alpha_{j+1}}\}$
$D \geq M_I$	$B_s^* = \frac{M_I}{\alpha_I}$	$B_l^* = D - \frac{M_I\alpha}{\alpha_I}$

choose the risk-free return as a benchmark to evaluate their investment performances [36]. Here, we choose the maximum profit that the operator can achieve without sensing (hence a risk free choice) as the reference point. This corresponds to the operator leasing a bandwidth $B_l = D$ and choosing $B_s = 0$, which leads to the profit of

$$R_p = D(\pi - c_l). \tag{11}$$

Substituting (11) into (10), we solve problem (10) and summarize the key result in Table II. To understand Table II, we first define some notations. We define $\hat{i} \in \mathcal{I}$ as the unique index that satisfies both the constraints $\alpha_{\hat{i}} \leq \frac{c_s}{c_l}$ and $\alpha_{\hat{i}+1} > \frac{c_s}{c_l}$[14]. We define H_j (for $j = \hat{i}+1, ..., I-1$) (see (17) in Appendix A) and M_j (for $j = \hat{i}+1, ..., I$) (see (15) and (16) in Appendix A) in Table II as decision indicators. The decision indicators are increasing functions of the leasing cost c_l and the risk parameter for gain β, and decreasing functions of the sensing cost c_s, the risk parameter for loss γ, and the loss penalty parameter λ. In other words, when the sensing cost c_s is higher or when the operator is more risk-averse (e.g., with a larger λ, a smaller β, or a larger γ), the decision indicators H_j and M_j decrease. The function $g_j(B_s)$ (for $j = \hat{i}+1, ..., I-1$) (see (27) in Appendix A) is a decreasing function in B_s.

Theorem 1. *Under Assumptions 1 and 2, the optimal sensing decision B_s^* for problem (10) and the optimal leasing decision B_l^* for problem (5) are summarized in Table II.*

By using the unimodal structure of Problem (10), we show that there is at most one inner local maximum point, and hence the global optimum is either at the local maximum point or at the boundaries [40]. For the detailed proof of Theorem 1, please refer to Appendix A. As shown in Table II, the operator's optimal sensing and leasing decisions depend on the decision indicators H_j and M_j. Notice that $M_j < H_j < M_{j+1}$ for every j, and all H_j (for $j = \hat{i}+1, ..., I-1$) and M_j (for $j = \hat{i}+1, ..., I$) are increasing in c_l and β, and are decreasing in c_s, γ, and λ. For a more risk-averse operator (with larger λ, smaller β, and larger γ), it has smaller decision indicators H_j and M_j (which refers to a lower row in Table II), hence it leads to a smaller B_s^*.

To better illustrate the insights behind Table II, we further characterize the impact of sensing cost c_s and the risk parameters λ, β and γ on B_s^* in the following corollaries.

Corollary 1. *The optimal sensing decision B_s^* for problem (10) is decreasing in the loss penalty parameter λ in (3) and the risk parameter for loss γ in (3).*

The proof of Corollary 1 is given in Appendix B. Corollary 1 indicates that if an operator is more risk-averse (with a larger loss penalty parameter λ or a larger risk parameter for loss γ), it will sense less, as it prefers avoiding loss due to a low sensing realization to achieving gain due to a high sensing realization.

Corollary 2. *When the demand is larger than the Ith decision indicator (i.e., $D > M_I$), the optimal sensing decision B_s^* for problem (10) is increasing in the risk parameter for gain β in (3).*

The proof of Corollary 2 is given in Appendix C. Corollary 2 indicates that for the case of a large demand (i.e., $D > M_I$), a more risk-seeking operator (with a larger risk parameter for gain β) will sense more to achieve a larger gain.

However, in the small demand case (i.e., $D \leq M_I$), as long as the total available spectrum from sensing can satisfy the demand (i.e., $B_s\alpha \geq D$), a larger sensing decision B_s leads to a constant revenue $D\pi$ but a larger total sensing cost $B_s c_s$, hence a less profit. Therefore, the optimal sensing decision B_s^* is not always increasing with β when $D \leq M_I$.

Corollary 3. *The optimal sensing decision B_s^* for problem (10) is decreasing in the sensing cost c_s.*

The proof of Corollary 3 is given in Appendix D. Corollary 3 indicates that the operator is more willing to sense when the sensing cost decreases.

For comparison, we also consider the operator's optimal sensing and leasing decisions under the EUT model. The detailed discussion is given in Appendix E.

V. SPECIAL CASE: OPTIMAL SENSING DECISION WITH BINARY OUTCOMES

In Section IV, we have focused on the discussion of the impact of the parameters of the s-shaped value function. In this section, we consider a special case with binary sensing outcomes (i.e., $I = 2$), to further illustrate the impact of reference point and probability distortion on the sensing decision. More specifically, the binary results are $\alpha_1 = 0$ and $\alpha_2 = 1$ with probabilities p_1 and p_2 as in (8) respectively, where $p_1 + p_2 = 1$.

A practical motivation of this case is the spectrum utilization at those areas such as the subway stations or overpasses, where the traffic patterns of PCs follow a very high peak-valley ratio [25], [26]. In these areas, there is hardly any spectrum left for the virtual operator when the traffic is at its peak, but the situation completely changes during the off-peak hours. Another example is the spectrum used by a rotating radar system [41], where the radar antenna gain and radiation pattern seen by the operator vary in a very high peak-valley ratio

---

[14]Both the case $\alpha_1 \geq \frac{c_s}{c_l}$ and the case $\alpha_I \leq \frac{c_s}{c_l}$ are trivial, and the discussion under these two cases are covered in the discussions under the case $\alpha_1 < \frac{c_s}{c_l} < \alpha_I$.

TABLE III
OPTIMAL SENSING DECISION UNDER DIFFERENT μ

Condition	Optimal Sensing Decision B_s^*
$\frac{c_l}{c_s} \leq \left(\frac{w(p_1)}{w(p_2)}\right)^{\frac{1}{\beta}} + 1$	$B_s^* = 0$
$\frac{c_l}{c_s} > \left(\frac{w(p_1)}{w(p_2)}\right)^{\frac{1}{\beta}} + 1$	$B_s^* = D$

TABLE IV
OPTIMAL SENSING DECISION B_s^* UNDER $R_p^{\text{HIGH}} = D(\pi - c_s)$ AND
$R_p^{\text{LOW}} = D(\pi - c_l - c_s)$

Condition	B_s^* under R_p^{high} (i.e., Risk-Seeking)	B_s^* under R_p^{low} (i.e., Risk-Averse)
$\frac{c_l}{c_s} < 1 + \frac{w(p_1)}{w(p_2)}$	$B_s^* = U_{RPH}^{'-1}(0)$	$B_s^* = 0$
$\frac{c_l}{c_s} \geq 1 + \frac{w(p_1)}{w(p_2)}$	$B_s^* = D$	$B_s^* = U_{RPL}^{'-1}(0)$

with the rotation of main beam. Hence, there are periods of time where the sensing realization is very high, and other periods of time when the sensing realization is very low. To better illustrate the impact of reference point and probability distortion, we consider the case $\beta = \gamma$ in this section to simplify the analysis[15]. Hence, by plugging $I = 2$ into (9), we can obtain the utility function:

$$U(B_s) = w(p_1)v(\pi D - B_s c_s - D c_l - R_p)$$
$$+ w(p_2)v(\pi D - B_s c_s - \max\{0, D - B_s\}c_l - R_p). \quad (12)$$

A. Impact of Probability Distortion

First, we discuss the impact of probability distortion on the operator's optimal sensing decision B_s^*. To compute the optimal sensing decision, we consider the same reference point $R_p = D(\pi - c_l)$ as in Section IV-B, and obtain the following theorem.

Theorem 2. *For the case of binary outcomes, under Assumptions 1 and 2, the optimal sensing decision B_s^* for problem (10) is summarized in Table III.*

The proof of Theorem 2 is given in Appendix F. The results in Table III depend on the ratio $w(p_1)/w(p_2)$. The operator will sense $B_s^* = D$ when the leasing and sensing cost ratio c_l/c_s exceeds the sensing threshold $[w(p_1)/w(p_2)]^{\frac{1}{\beta}} + 1$, and will sense $B_s^* = 0$ otherwise. Since $p_1 + p_2 = 1$, according to the probability distortion effect in PT, the larger probability is underweighed and the smaller probability is overweighed. From Table III, for the case $p_1 < p_2$, p_1 is overweighted and p_2 is underweighted in PT (i.e., $w(p_1)/w(p_2) > p_1/p_2$), where the operator *underestimates* the chance of having a high sensing realization. Thus, the PT operator is more risk-averse and will sense less than or equal to an EUT operator because it has a higher sensing threshold. On the other hand, when $p_1 > p_2$, p_2 is overweighted (i.e., $w(p_1)/w(p_2) < p_1/p_2$), where the operator *overestimates* the chance of a high sensing realization. Thus, the PT operator is more risk-seeking and will sense larger than or equal to that of an EUT operator because the PT operator has a lower sensing threshold.

B. Impact of Reference Point

Next, we discuss the impact of reference point R_p on the operator's optimal sensing decision B_s^*. A high reference point R_p indicates that the operator has a high expectation on the profit, and it is more likely to experience a *loss* since the outcome is often less than its expectation. On the other hand, a low reference point R_p indicates that the operator has a low expectation, and it is more likely to experience a *gain* since

[15]We do not obtain additional new insights on reference point and probability distortion in the case $\beta \neq \gamma$, hence we omit the discussion of $\beta \neq \gamma$ here.

the outcome is often beyond its expectation. As we will see in the following, whether an outcome is considered as a loss or a gain can significantly affect the operator's subjective valuation of the outcome, and hence its sensing decision.

To better illustrate the impact of reference point, we focus on two choices: (i) A high reference point $R_p^{\text{high}} = D(\pi - c_s)$, which reflects the operator's expectation of realizing all the sensing spectrum D. (ii) the low reference point $R_p^{\text{low}} = D(\pi - c_l - c_s)$, which reflects the operator's expectation of not realizing any of the sensing spectrum D. In other words, the same outcome is more likely to be considered as a loss under the high reference point than under the low reference point.

From (12), we obtain the utility under the high reference point as

$$U_{RPH}(B_s) = -\lambda w(p_1)(B_s c_s + D c_l - D c_s)^{\beta}$$
$$- \lambda w(p_2)[D(c_l - c_s) - B_s(c_l - c_s)]^{\beta}, \quad (13)$$

and the utility under the low reference point as

$$U_{RPL}(B_s) = w(p_1)(D c_s - B_s c_s)^{\beta} + w(p_2)[B_s(c_l - c_s) + D c_s]^{\beta}. \quad (14)$$

By studying the first order derivatives under the two reference points $U'_{RPH}(B_s)$ and $U'_{RPL}(B_s)$, we can compute the optimal sensing decision that solves problem (10) in the following theorem.

Theorem 3. *For the case of binary outcomes, under Assumptions 1 and 2, the optimal sensing decision B_s^* for problem (10) under different reference points $R_p^{high} = D(\pi - c_s)$ and $R_p^{low} = D(\pi - c_l - c_s)$ are summarized in Table IV.*

The proof of Theorem 3 is given in Appendix G. Theorem 3 indicates that B_s^* under R_p^{high} is always larger than B_s^* under R_p^{low}. This means that an operator with R_p^{high} is more willing to sense compared to an operator with R_p^{low}. When an operator has a high expectation (due to a high reference point), it is more likely to encounter losses than gains under uncertainty. Since the operator's valuation function $v(x - R_p)$ is convex in the loss region, it will sense more in order to gain more in the case of high sensing realization (i.e., $\alpha = 1$). In contrast, when an operator has a low expectation (due to a low reference point), it is more likely to encounter gains than losses. Since the operator's valuation function $v(x - R_p)$ is concave in terms of gains, it will sense less, in order to avoid the risk of low sensing realization (i.e., $\alpha = 0$). To summarize, an operator who expects a higher profit is more risk-seeking, and an operator who expects a lower profit is more risk-averse.

VI. PERFORMANCE EVALUATIONS

In this section, we illustrate the operator's optimal sensing decision and the corresponding expected profit under different
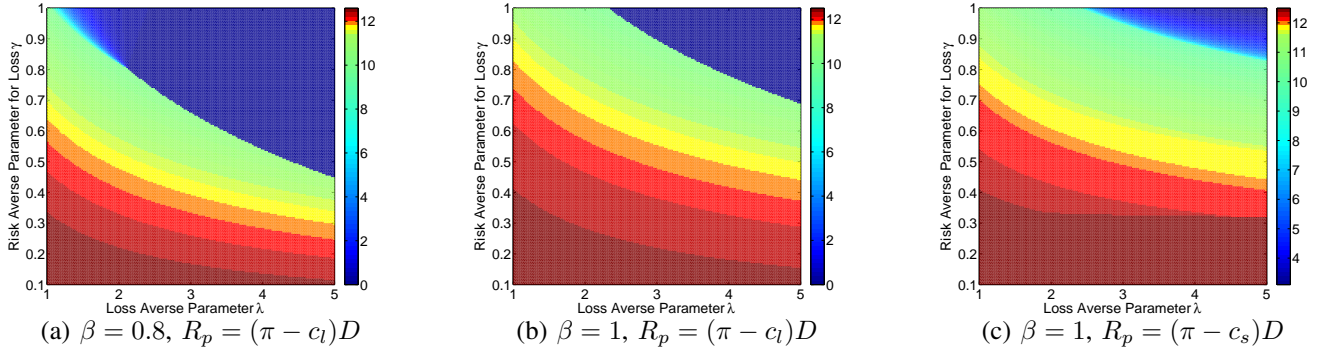
(a) $\beta = 0.8$, $R_p = (\pi - c_l)D$ (b) $\beta = 1$, $R_p = (\pi - c_l)D$ (c) $\beta = 1$, $R_p = (\pi - c_s)D$

Fig. 3.   Optimal sensing decision B_s^* versus γ and λ for different β and R_p. Other parameters are $c_l = 5$, $c_s = 2$, and $D = 10$. (The color represents optimal sensing decision B_s^*.)

system parameters. The key insights under the PT modeling include: (a) A *risk-averse* operator will sense less and lease more, which leads to a smaller profit with a lower risk of loss; while a *risk-seeking* operator will sense more and lease less, which leads to a larger profit with a higher risk of loss. (b) *Risk preference* changes with the probability of high sensing realization. When the probability of high sensing realization changes from very high to very low, the operator changes from risk-averse to risk-seeking. (c) Both *risk-averse* and *risk-seeking* operators face a tradeoff between satisfying their risk preferences and maximizing expected profit. A *risk-averse* operator achieves a better tradeoff in a high sensing cost scenario than in a low sensing cost scenario, while a *risk-seeking* operator achieves a better tradeoff in a low sensing cost scenario than in a high sensing cost scenario.

A. Evaluation of the Optimal Sensing Decision

We first evaluate the impact of the three characteristics of PT on the operator's optimal decision.

1) Impact of s-shaped Value Function: First, we illustrate the operator's optimal sensing decision under different parameters of s-shaped value function (i.e., γ, β, and λ), assuming reference point $R_p = (\pi - c_l)D$ and linear probability distortion (i.e., $\mu = 1$). We compare the optimal sensing decision and the corresponding expected profit with the EUT benchmark, where $\lambda = \beta = \gamma = 1$.

First, in Fig. 3(a) and Fig. 3(b), we study the optimal sensing decision B_s^* against the loss penalty parameter λ and the risk averse parameter for loss γ. To illustrate the impact of β, we set $\beta = 0.8$ in Fig. 3(a) and $\beta = 1$ in Fig. 3(b). The other system parameters are fixed at $c_l = 5$, $c_s = 2$, and $D = 10$. We observe the behaviors of both risk-averse and risk-seeking operators in Fig. 3(a) and Fig. 3(b). The upper right parts of the figures correspond to the risk-averse operators, and the lower left parts of the figures are risk-seeking operators. The EUT benchmark corresponds to the case of $\lambda = \beta = \gamma = 1$ (i.e., upper left corners of Fig. 3(b) and Fig. 3(c)). We observe that risk-averse operators sense less and risk-seeking operators sense more.

Impact of γ on B_s^*: We can see that for fixed β and λ, the operator senses more when γ decreases (see y-axis in Fig. 3(a) and Fig. 3(b)), as stated in Corollary 1. The intuition is that when γ decreases from 1 (hence the operator is more risk-seeking than an EUT operator), the operator experiences

less marginal disutility from loss. In order to win a potentially large gain, the operator is more willing to take risk and sense more. An example to illustrate this impact is that a gambler, who has already lost a lot, cares less of losing an additional \$1 than a gambler who just starts to gamble.

Impact of λ on B_s^*: As stated in Corollary 1, for fixed γ and β, the operator senses less when λ increases (see the x-axis in Fig. 3(a) and Fig. 3(b)). The intuition is that when λ is larger, the penalty of loss to the operator is larger (hence the operator is more risk-averse than an EUT operator). In order to avoid a potential loss, the operator will sense less.

Impact of β on B_s^*: By comparing Fig. 3(a) and Fig. 3(b), we can observe that the operator senses more when β increases for fixed λ and γ, which verifies Corollary 2. The intuition is that when β decreases from 1 (hence the operator is more risk-averse than an EUT operator), the operator experiences less marginal utility from the same gain. Hence, the operator will sense less to achieve a certain gain, rather than taking risk for a very large gain. An example to illustrate this impact is that a rich man is less willing to earn an additional \$1 than a poor man if doing so requires a fixed amount of effort.

2) Impact of Reference Point: In Fig. 3(b), we have considered the reference point of $R_p = D(\pi - c_l)$. Next, we further illustrate the operator's optimal sensing decision under another high reference point of $R_p = D(\pi - c_s)$. As stated in Section V-B, whether an outcome is considered a loss and gain will significantly affect the operator's subjective valuation of the outcome, hence will affect its sensing decision.

In Fig. 3(c), we consider the case of $R_p = D(\pi - c_s)$, which reflects the operator's expectation of realizing all of the sensing spectrum D. Hence the same outcome is more likely to be considered as a loss under $R_p = D(\pi - c_s)$ than under $R_p = D(\pi - c_l)$. We plot the optimal sensing decision of the risk-seeking and risk-averse operators for different values of λ and γ. The other system parameters are the same as those in Fig. 3(b). By comparing Fig. 3(b) with Fig. 3(c), we observe that the operator with a low reference point $R_p = D(\pi - c_l)$ senses less. The intuition is that when an operator has a low reference point, it has a low expectation, so it is more likely to encounter gains than losses. Due to the concavity of its valuation function $v(x - R_p)$ in gain, the operator will become more risk-averse and will sense less to avoid the risk of low sensing realization.

3) Impact of Probability Distortion: Then, we illustrate the operator's optimal sensing decision under different probability
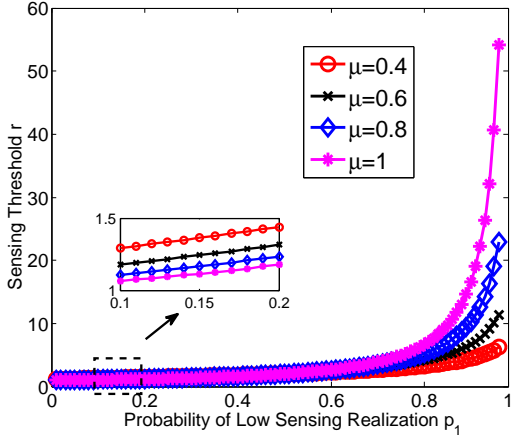
Fig. 4. Sensing threshold r versus probability of low sensing realization p_1 with different probability distortion parameter μ for $\beta = \gamma = \lambda = 1$, and $R_p = D(\pi - c_l)$.
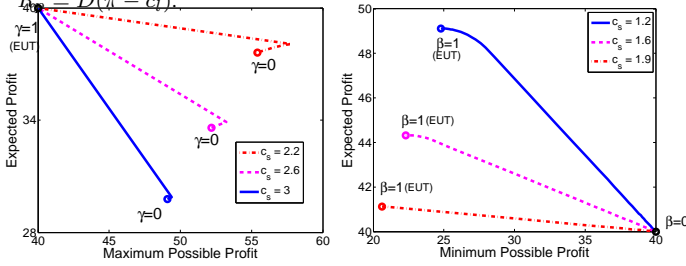

Fig. 5. (a) Tradeoff between optimal expected profit and maximum possible profit for $\beta = 1$ under different c_s and γ. (b) Tradeoff between optimal expected profit and minimum possible profit for $\gamma = 1$ under different c_s and β. Other parameters are $R_p = (\pi - c_l)D$, $c_l = 4$, $\pi = 8$, and $D = 10$.

distortion parameters μ for the case of binary sensing outcomes (i.e., $I = 2$). We compare the result with the non-distorted benchmark, where $\mu = 1$. The PT operator is *risk-seeking* when the probability of low sensing realization p_1 is high, and it is *risk-averse* when p_1 is low.

We notice that the operator's decisions can be characterized by a threshold r related to the leasing and sensing cost ratio $\frac{c_l}{c_s}$. When $\frac{c_l}{c_s} \geq r$, meaning that leasing is expensive, the operator will choose to sense for all the demand D. Otherwise, when $\frac{c_l}{c_s} < r$, the operator will sense less than the demand D and lease for part of the demand[16]. Hence, a larger r means that the operator is less willing to sense.

In Fig. 4, we plot the sensing threshold r against p_1 for different values of μ, where we assume $\beta = \gamma = \lambda = 1$, and $R_p = D(\pi - c_l)$. We can see that the threshold r decreases in μ when $p_1 < 0.5$, and increases in μ when $p_1 > 0.5$. As a smaller μ means that the operator will overweigh the low probability more, it becomes more risk-averse when p_1 is small. Similarly, since a smaller μ means that the operator will underweigh the high probability more, it is more risk-seeking when p_1 is large.

B. Expected Profit and Risk Preference Tradeoff

We then evaluate the tradeoff between the expected profit and risk preference of an operator. A risk-seeking operator is

[16]Notice that the threshold r is different under different scenarios. For example, with $R_p = D(\pi - c_l)$ for binary sensing outcomes, we have $r = [w(p_1)/w(p_2)]^{\frac{1}{\beta}} + 1$ from Theorem 2. On the other hand, with $R_p = D(\pi - c_s)$ for binary sensing outcomes, we have $r = 1 + w(p_1)/w(p_2)$ from Theorem 3.

aggressive and mainly interested in earning a high maximum profit, while a risk-averse operator is conservative and mainly interested in guaranteeing a high minimum profit. Given the system parameters (i.e., c_s, c_l, π, and D) and risk perference parameters (i.e., λ, β, and γ), we let B_s^* and B_l^* be the optimal sensing and leasing decisions discussed in Section IV. The optimal expected profit $\mathbb{E}_\alpha[R(B_s^*, B_l^*, \alpha)]$ is the averaged profit over different sensing realizations. The maximum possible profit $R(B_s^*, B_l^*, 1)$ is the profit with $\alpha = 1$, and the minimum possible profit $R(B_s^*, B_l^*, 0)$ is the profit with $\alpha = 0$.

Tradeoff of a risk-seeking operator: In Fig. 5(a), we plot the tradeoff between the expected profit and the maximum possible profit for $\beta = 1$ under different c_s and γ. Since an EUT operator ($\gamma = 1$) makes decision only by maximizing expected profit, we can see from Fig. 5(a) that it can achieve the highest expected profit. On the other hand, a PT operator makes decision by taking into account both the expected profit and its risk preference. More specifically, although a risk-seeking PT operator (i.e., $\gamma < 1$) achieves a lower expected profit comparing to an EUT operator, it can earn a higher maximum possible profit than an EUT operator. Notice in Fig. 5(a), when the operator is very risk-seeking ($\gamma \to 0$), the expected profit and maximum possible profit both decrease. This is because the operator can achieve the maximum possible profit when the sensed spectrum is fully realized. However, when the sensing decision B_s^* is larger than demand D (hence the maximum realized spectrum is larger than D), being more risk-seeking (which leads to a larger sensing decision B_s^*) will not lead to a larger maximum possible profit, but will only lead to a larger probability of achieving that maximum possible profit. This explains the "bending" in the figure. From Fig. 5(a), we also observe that the tradeoff varies with sensing cost c_s. We can see that under the three cases of c_s, an EUT operator has the same expected profit and maximum possible profit, because it has the same optimal sensing decision ($B_s^* = 0$). However, a risk-seeking operator will have a smaller loss in expected profit but a larger gain in maximum possible profit than an EUT operator ($\gamma = 1$) when the sensing cost c_s decreases. In other words, a risk-seeking operator achieves a better tradeoff when the sensing cost decreases.

Tradeoff of a risk-averse operator: In Fig. 5(b), we plot the tradeoff between optimal expected profit and minimum possible profit for $\gamma = 1$ under different c_s and β. We can see from Fig. 5(b) that a risk-averse operator ($\beta < 1$) achieves a lower expected profit comparing to an EUT operator ($\beta = 1$), but guarantees a higher minimum possible profit than an EUT operator. For example, an extremely risk-averse operator ($\beta \to 0$) has a similar expected profit and minimum possible profit under any sensing cost c_s, because its optimal sensing decision B_s^* is always close to zero. We can also observe that a risk-averse operator will have a smaller loss in expected profit but a larger gain in minimum possible profit than an EUT operator when the sensing cost c_s increases. In other words, a risk-averse operator achieves a better tradeoff when the sensing cost increases.

VII. Conclusions and Future Work

In this paper, we considered a spectrum investment problem with sensing uncertainty, where an operator decides its spectrum sensing and leasing decisions by considering both expected profit and its risk preference based on prospect theory. This is the first paper that studied the optimal decisions based on all three characteristics of prospect theory in the wireless communication literature, and compared and contrasted these decisions with those under the more widely used expected utility theory. Our results suggested that a risk-averse operator can achieve a large expected profit while guaranteeing a satisfactory level of minimum possible profit when the sensing cost is high. On the other hand, a risk-seeking operator can achieve both a large expected profit and maximum possible profit when the sensing cost is low.

This study demonstrated that a more realistic modeling based on prospect theory is important in understanding the operator's decisions in the wireless industry. On the other hand, this study is only a small first step, as we have only considered the operator's decision in a single time slot. Regarding the future work, we will consider a more general problem with decisions to be made in multiple time slots. In such a model, the operator's reference point may change over time, and the study of dynamic reference point is a recent active research field in prospect theory [17], [42]. We will also conduct a survey to evaluate different people's risk preferences.

References

[1] J. Yu, M. H. Cheung, and J. Huang, "Spectrum investment with uncertainty based on prospect theory," in *Proc. of IEEE ICC*, Sydney, Australia, June 2014.

[2] Dataxoom, "What are MVNOs and why do they exist?" http://dataxoom.com/blog/2015/05, May 2015.

[3] Transparency Market Research, "Mobile virtual network operator (mvno) market - Global industry analysis, size, share, growth, trends and forecast 2015 - 2023," Feb. 2016.

[4] Consumer Cellular, https://www.consumercellular.com.

[5] Cisco, "MVNOs and MVNEs: Simple, automated, cost effective deployments," White Paper, Oct. 2015.

[6] T. Yucek and H. Arslan, "A survey of spectrum sensing algorithms for cognitive radio applications," *IEEE Communications Surveys Tutorials*, vol. 11, no. 1, pp. 116–130, Jan. 2009.

[7] Y.-C. Liang, Y. Zeng, E. Peh, and A. T. Hoang, "Sensing-throughput tradeoff for cognitive radio networks," *IEEE Transactions on Wireless Communications*, vol. 7, no. 4, pp. 1326–1337, Apr. 2008.

[8] K. Zhu, D. Niyato, P. Wang, and Z. Han, "Dynamic spectrum leasing and service selection in spectrum secondary market of cognitive radio networks," *IEEE Transactions on Wireless Communications*, vol. 11, no. 3, pp. 1136–1145, Mar. 2012.

[9] L. Duan, J. Huang, and B. Shou, "Duopoly competition in dynamic spectrum leasing and pricing," *IEEE Transactions on Mobile Computing*, vol. 11, no. 11, pp. 1706–1719, Nov. 2012.

[10] G. S. Kasbekar and S. Sarkar, "Spectrum auction framework for access allocation in cognitive radio networks," *IEEE/ACM Transactions on Networking*, vol. 18, no. 6, pp. 1841–1854, Dec. 2010.

[11] L. Gao, X. Wang, Y. Xu, and Q. Zhang, "Spectrum trading in cognitive radio networks: A contract-theoretic modeling approach," *IEEE Journal of Selected Areas in Communications*, vol. 29, no. 4, pp. 843–855, Apr. 2011.

[12] H. Jin, G. Sun, X. Wang, and Q. Zhang, "Spectrum trading with insurance in cognitive radio networks," in *Proc. of IEEE Infocom*, Orlando, Mar. 2012.

[13] L. Duan, J. Huang, and B. Shou, "Investment and pricing with spectrum uncertainty: A cognitive operator's perspective," *IEEE Trans. on Mobile Computing*, vol. 10, no. 11, pp. 1590–1604, Nov. 2011.

[14] D. Kahneman and A. Tversky, "Prospect theory: An analysis of decision under risk," *Econometrica*, vol. 47, no. 2, pp. 263–291, Mar. 1979.

[15] A. Tversky and D. Kahneman, "Advances in prospect theory: Cumulative representation of uncertainty," *Journal of Risk and Uncertainty*, vol. 5, no. 4, pp. 297–323, Oct. 1992.

[16] D. Kahneman and A. Tversky, *Choices, Values, and Frames*. New York: Cambridge University Press, 2000.

[17] H. Jin and X. Zhou, "Behavioral portfolio selection in continuous time," *Mathematical Finance*, vol. 18, no. 3, pp. 385–426, July 2008.

[18] D. Hubert and D. Wolfgang, "Portfolio insurance and prospect theory investors: Popularity and optimal design of capital protected financial products," *Journal of Banking & Finance*, vol. 35, no. 7, pp. 1683–1697, 2011.

[19] B. Jeffrey, "Model building with prospect theory: A cognitive approach to international relations," *Political Psychology*, vol. 23, no. 4, pp. 759–786, 2002.

[20] C. F. Camerer and G. Loewenstein, *Advances in behavioral economics*. Princeton: Princeton University Press, 2004.

[21] T. Li and N. B. Mandayam, "When users interfere with protocols: Prospect theory in wireless networks using random access and data pricing as an example," *IEEE Trans. on Wireless Communications*, vol. 13, no. 4, pp. 1888–1907, Apr. 2014.

[22] Y. Yang, L. Park, N. Mandayam, I. Seskar, A. Glass, and N. Sinha, "Prospect pricing in cognitive radio networks," *IEEE Transactions on Cognitive Communications and Networking*, vol. 1, no. 1, pp. 56–70, Mar. 2015.

[23] Y. Wang, W. Saad, N. B. Mandayam, and H. V. Poor, "Integrating energy storage into the smart grid: A prospect theoretic approach," in *Proc. of IEEE ICASSP*, Florence, May 2014.

[24] L. Xiao, N. B. Mandayam, and H. V. Poor, "Prospect theoretic analysis of energy exchange among microgrids," *IEEE Transactions on Smart Grid*, vol. 6, no. 1, pp. 63–72, June 2015.

[25] H. Wang, J. Ding, Y. Li, P. Hui, J. Yuan, and D. Jin, "Characterizing the spatio-temporal inhomogeneity of mobile traffic in large-scale cellular data networks," in *Proc. of 7th HotPOST*, Hangzhou, 2015.

[26] H. Wang, F. Xu, Y. Li, P. Zhang, and D. Jin, "Understanding mobile traffic patterns of large scale cellular towers in urban environment," in *Proc. of ACM IMC*, Tokyo, Japan, Oct. 2015.

[27] Y.-C. Liang, Y. Zeng, E. C. Peh, and A. T. Hoang, "Sensing-throughput tradeoff for cognitive radio networks," *IEEE Transactions on Wireless Communications*, vol. 7, no. 4, pp. 1326–1337, Apr. 2008.

[28] S. Li, J. Huang, and S.-Y. R. Li, "Dynamic profit maximization of cognitive mobile virtual network operator," *IEEE Transactions on Mobile Computing*, vol. 13, no. 3, pp. 526–540, Mar. 2014.

[29] D. Willkomm, S. Machiraju, J. Bolot, and A. Wolisz, "Primary users in cellular networks: A large-scale measurement study," in *Proc. of IEEE DySPAN*, Chicago, Oct. 2008.

[30] ——, "Primary user behavior in cellular networks and implications for dynamic spectrum access," *IEEE Communications Magazine*, vol. 47, no. 3, pp. 88–95, Mar. 2009.

[31] S. Geirhofer, L. Tong, and B. M. Sadler, "Dynamic spectrum access in wlan channels: Empirical model and its stochastic analysis," in *Proc. of ACM TAPAS*, Boston, Aug. 2006.

[32] H. Kim and K. G. Shin, "Efficient discovery of spectrum opportunities with mac-layer sensing in cognitive radio networks," *IEEE Transactions on Mobile Computing*, vol. 7, no. 5, pp. 533–545, May 2008.

[33] X. Chen and J. Huang, "Evolutionarily stable spectrum access," *IEEE Transactions on Mobile Computing*, vol. 12, no. 7, pp. 1281–1293, July 2013.

[34] C. Tekin and M. Liu, "Approximately optimal adaptive learning in opportunistic spectrum access," in *Proc. of IEEE Infocom*, Orlando, Mar. 2012.

[35] O. Korcak, G. Iosifidis, T. Alpcan, and I. Koutsopoulos, "Operator collusion and market regulation policies for wireless spectrum management," *IEEE Transactions on Mobile Computing*, to appear, 2016.

[36] X. D. He and X. Y. Zhou, "Portfolio choice under cumulative prospect theory: An analytical treatment," *Management Science*, vol. 57, no. 2, pp. 315–331, Feb. 2011.

[37] M. O. Rieger and M. Wang, "Prospect theory for continuous distributions," *Journal of Risk and Uncertainty*, vol. 36, no. 1, pp. 83–102, Jan. 2008.

[38] A. Mas-Colell, M. D. Whinston, and J. R. Green, *Microeconomic Theory*. Oxford University Press, 1995.

[39] Y. Zeng, Y.-C. Liang, A. T. Hoang, and R. Zhang, "A review on spectrum sensing techniques for cognitive radio: challenges and solutions," *EURASIP Journal on Advances in Signal Processing*, pp. 1–15, 2010.

[40] S. Dharmadhikari and K. Joag-Dev, *Unimodality, convexity, and applications*. New York: Elsevier, 1988.

[41] R. Saruthirathanaworakun, J. M. Peha, and L. M. Correia, "Opportunistic sharing between rotating radar and cellular," *IEEE Journal on Selected Areas in Communications*, vol. 30, no. 10, pp. 1900–1910, Nov. 2012.

[42] G. Yin and X. Zhou, "Markowitz's mean-variance portfolio selection with regime switching: From discrete-time models to their continuous-time limits," *IEEE Transactions on Automatic Control*, vol. 49, no. 3, pp. 349–360, Mar. 2004.

APPENDIX

A. Proof of Theorem 1

In this proof, we divide the feasible range of B_s into three intervals, $\left[0, \frac{D}{\alpha_I}\right]$, $\left[\frac{D}{\alpha_I}, \frac{Dc_l}{c_s}\right]$, and $\left(\frac{Dc_l}{c_s}, \infty\right)$, and analyze the optimal decision B_s^* in each interval. By this division, in the interval $\left[0, \frac{D}{\alpha_I}\right]$, $B_s\alpha_i \leq D$ for all $i \in \mathcal{I}$, so that we do not need to consider the possibility of sensing realization exceeds the demand. In the interval $\left(\frac{Dc_l}{c_s}, \infty\right)$, we have $Dc_l < B_s c_s$, which means that the total cost of sensing $B_s c_s$ will be larger than the cost of leasing only Dc_l. Hence the optimal solution will not be in this range. The above reason leads to the division of three intervals.

We will use the following notations in the proof:

$$M_I \triangleq \left[\frac{\sum_{i=\hat{\imath}+1}^{I}(c_l\alpha_i - c_s)^\beta w(p_i)\beta}{\sum_{i=1}^{\hat{\imath}}\lambda\gamma(c_s - c_l\alpha_i)^\gamma \left(\frac{1}{\alpha_I}\right)^{\gamma-\beta}w(p_i)}\right]^{\frac{1}{\gamma-\beta}}, \quad (15)$$

$$M_j \triangleq \left[\frac{\sum_{i=\hat{\imath}+1}^{j}(c_l\alpha_i - c_s)^\beta w(p_i)\beta - \beta c_s(c_l\alpha_j - c_s)^{\beta-1}\sum_{i=j+1}^{I}w(p_i)}{\sum_{i=1}^{\hat{\imath}}\lambda\gamma(c_s - c_l\alpha_i)^\gamma \left(\frac{1}{\alpha_j}\right)^{\gamma-\beta}w(p_i)}\right]^{\frac{1}{\gamma-\beta}},$$
$$j = \hat{\imath}+1, \hat{\imath}+2, ..., I-1, \quad (16)$$

and

$$H_j \triangleq \left[\frac{\sum_{i=\hat{\imath}+1}^{j}(c_l\alpha_i - c_s)^\beta w(p_i)\beta - \beta c_s(c_l\alpha_{j+1} - c_s)^{\beta-1}\sum_{i=j+1}^{I}w(p_i)}{\sum_{i=1}^{\hat{\imath}}\lambda\gamma(c_s - c_l\alpha_i)^\gamma \left(\frac{1}{\alpha_{j+1}}\right)^{\gamma-\beta}w(p_i)}\right]^{\frac{1}{\gamma-\beta}},$$
$$j = \hat{\imath}+1, \hat{\imath}+2, ..., I-1. \quad (17)$$

Next, we analyze the optimal decision B_s^* within each interval.

Case I: $B_s \in \left[0, \frac{D}{\alpha_I}\right]$. We first compute the optimal decision B_s^* in this interval using the first order condition. In this case, $B_s\alpha_i \leq D$ for all $i \in \mathcal{I}$, so the optimal leasing decision $B_l^* = D - B_s\alpha_i \geq 0$. From (7), the revenue is

$$R(B_s, B_l^*, \alpha_i) = (\pi - c_l)D - B_s c_s + B_s c_l \alpha_i. \quad (18)$$

Since α_i follows a discrete distribution in $[0, 1]$, we can plug (18) into (9), and get (19) by taking the proper expectation.

$$U(B_s) = \sum_{i=\hat{\imath}+1}^{I}(B_s c_l \alpha_i - B_s c_s)^\beta w(p_i) - \sum_{i=1}^{\hat{\imath}}\lambda(B_s c_s - B_s c_l \alpha_i)^\gamma w(p_i)$$
$$= \sum_{i=\hat{\imath}+1}^{I}(c_l\alpha_i - c_s)^\beta w(p_i)B_s^\beta - \sum_{i=1}^{\hat{\imath}}\lambda(c_s - c_l\alpha_i)^\gamma w(p_i)B_s^\gamma. \quad (19)$$

We consider the first order derivative of (19) with respect to B_s:

$$U'(B_s) = \sum_{i=\hat{\imath}+1}^{I}(c_l\alpha_i - c_s)^\beta w(p_i)\beta B_s^{\beta-1} - \sum_{i=1}^{\hat{\imath}}\lambda\gamma(c_s - c_l\alpha_i)^\gamma w(p_i)B_s^{\gamma-1}$$
$$= B_s^{\beta-1}\left[\sum_{i=\hat{\imath}+1}^{I}(c_l\alpha_i - c_s)^\beta w(p_i)\beta - \sum_{i=1}^{\hat{\imath}}\lambda\gamma(c_s - c_l\alpha_i)^\gamma w(p_i)B_s^{\gamma-\beta}\right]. \quad (20)$$

We can obtain

$$U'(B_s) > 0 \Leftrightarrow \sum_{i=1}^{\hat{\imath}} -\lambda\gamma(-c_l\alpha_i + c_s)^\gamma w(p_i)B_s^{\gamma-\beta}$$
$$+ \sum_{i=\hat{\imath}+1}^{I}(c_l\alpha_i - c_s)^\beta w(p_i)\beta > 0$$
$$\Leftrightarrow B_s < \left[\frac{\sum_{i=\hat{\imath}+1}^{I}(c_l\alpha_i - c_s)^\beta w(p_i)\beta}{\sum_{i=1}^{\hat{\imath}}\lambda\gamma(c_s - c_l\alpha_i)^\gamma w(p_i)}\right]^{\frac{1}{\gamma-\beta}} = \frac{M_I}{\alpha_I}, \quad (21)$$

where M_I is defined in (15). Since the second order derivative $U''(B_s) < 0$, we know that $U'(B_s)$ in (20) decreases in B_s. Hence, we only need to compare the right boundary $\frac{D}{\alpha_I}$ and the critical point $\frac{M_I}{\alpha_I}$. From (21), we have

$$B_s^* = \begin{cases} \frac{M_I}{\alpha_I}, & \text{if } \frac{M_I}{\alpha_I} < \frac{D}{\alpha_I}, \\ \frac{D}{\alpha_I}, & \text{if } \frac{M_I}{\alpha_I} \geq \frac{D}{\alpha_I}. \end{cases} \quad (22)$$

Intuitively, when the leasing cost c_l is high (and hence every H_j in (17) is large), the utility increases when the operator senses more (and leases less).

Case II: $B_s \in \left[\frac{D}{\alpha_I}, \frac{Dc_l}{c_s}\right]$. We compute the optimal decision B_s^* in this interval by capturing the unimodal structure. In this case, profit $R(B_s, B_l^*, \alpha)$ can be represented as a piecewise function as follows.

$$R(B_s, B_l^*, \alpha) = \begin{cases} \pi D - B_s c_s, & \text{if } \alpha > \frac{D}{B_s}, \\ B_s c_l \alpha - B_s c_s, & \text{if } 0 < \alpha < \frac{D}{B_s}. \end{cases} \quad (23)$$

We substitute (23) into (9), and the utility function becomes

$$U(B_s) = \sum_{i=1}^{\hat{\imath}} -\lambda[B_s(c_s - c_l\alpha_i)]^\gamma w(p_i)$$
$$+ \sum_{i=\hat{\imath}+1}^{j}[B_s(c_l\alpha_i - c_s)]^\beta w(p_i) + \sum_{i=j+1}^{I}(Dc_l - B_s c_s)^\beta w(p_i). \quad (24)$$

The value of j in (24) varies when B_s belongs to different sub-intervals. The utility function $U(B_s)$ in (24) is a continuous function in the whole interval, and is differentiable in each of the $I - \hat{\imath}$ sub-intervals, $\frac{D}{\alpha_{j+1}} \leq B_s \leq \frac{D}{\alpha_j}$, $j = \hat{\imath}+1$, ..., $I-1$, and $\frac{D}{\alpha_{\hat{\imath}+1}} \leq B_s \leq \frac{Dc_l}{c_s}$. Although the utility function is not globally differentiable, we can evaluate the derivative of each sub-interval, and find the optimal point for each of the $I - \hat{\imath}$ sub-intervals. Then we can find the optimal solution of the whole interval by comparing the optimal points in the $I - \hat{\imath}$ sub-intervals.

We conclude the optimal sensing decision $B_{s,j}^*$ in the interval $\frac{D}{\alpha_{j+1}} \leq B_s \leq \frac{D}{\alpha_j}$, $j = \hat{i}+1, ..., I-1$ in Proposition 1.

Proposition 1. *The maximum utility value $U\left(B_{s,j}^*\right)$ in each sub-interval among $\frac{D}{\alpha_{j+1}} \leq B_s \leq \frac{D}{\alpha_j}$, $j = \hat{i}+1, ..., I-1$ is achieved at*

$$B_{s,j}^* = \begin{cases} \dfrac{D}{\alpha_j}, & \text{if } D \leq M_j, \\ g_j^{-1}(0), & \text{if } M_j < D < H_j, \\ \dfrac{D}{\alpha_{j+1}}, & \text{if } H_j \leq D < M_{j+1}. \end{cases} \quad (25)$$

Proof: We prove Proposition 1 by capturing the unimodal structure of (24) in each sub-interval $\frac{D}{\alpha_{j+1}} \leq B_s \leq \frac{D}{\alpha_j}$. For a unimodal problem, the optimal point is either at the unique local maximum point or the boundaries. For $\frac{D}{\alpha_{j+1}} \leq B_s \leq \frac{D}{\alpha_j}$, we consider the first order derivative of (24) with respect to B_s:

$$U'(B_s) = \sum_{i=1}^{\hat{i}} -\lambda \left(c_s - c_l \alpha_i\right)^\gamma w(p_i) \gamma B_s^{\gamma-1}$$

$$+ \sum_{i=\hat{i}+1}^{j} \beta (c_l \alpha_i - c_s)^\beta w(p_i) B_s^{\beta-1} - c_s \sum_{i=j+1}^{I} \beta (D c_l - B_s c_s)^{\beta-1} w(p_i)$$

$$= \sum_{i=\hat{i}+1}^{j} \beta (c_l \alpha_i - c_s)^\beta w(p_i) B_s^{\beta-1} \left[\frac{\sum_{i=1}^{\hat{i}} -\lambda (c_s - c_l \alpha_i)^\gamma B_s^{\gamma-\beta}}{\sum_{i=\hat{i}+1}^{j} (c_l \alpha_i - c_s)^\beta w(p_i)\beta} \right.$$

$$\left. + 1 - \frac{c_s \sum_{i=j+1}^{I} \left(\frac{D c_l}{B_s} - c_s\right)^{\beta-1} w(p_i)}{\sum_{i=\hat{i}+1}^{j} (c_l \alpha_i - c_s)^\beta w(p_i)} \right], \quad (26)$$

where we define

$$g_j(B_s) \triangleq \frac{\sum_{i=1}^{\hat{i}} -\lambda (c_s - c_l \alpha_i)^\gamma B_s^{\gamma-\beta}}{\sum_{i=\hat{i}+1}^{j} (c_l \alpha_i - c_s)^\beta w(p_i)\beta} + 1$$

$$- \frac{c_s \left(\frac{D c_l}{B_s} - c_s\right)^{\beta-1} \sum_{i=j+1}^{I} w(p_i)}{\sum_{i=\hat{i}+1}^{j} (c_l \alpha_i - c_s)^\beta w(p_i)}, \quad j = \hat{i}+1, \hat{i}+2, ..., I-1. \quad (27)$$

With (27), we can rewrite $U'(B_s)$ as

$$U'(B_s) = \sum_{i=\hat{i}+1}^{j} \beta (c_l \alpha_i - c_s)^\beta w(p_i) B_s^{\beta-1} g_j(B_s), \quad (28)$$

where $\sum_{i=\hat{i}+1}^{j} \beta (c_l \alpha_i - c_s)^\beta w(p_i) B_s^{\beta-1} > 0$. The function $g_j(B_s)$ in (27) is a strictly decreasing function of B_s, which means the first order derivative $U'(B_s)$ in (28) will only be zero at most once, thus there is at most one local maximum point[17].

[17]If this point is local minimum, then there is no local maximum point, and the maximum point in this sub-interval is at the boundaries.

We then consider the two boundary points: $B_s = \frac{D}{\alpha_{j+1}}$ and $B_s = \frac{D}{\alpha_j}$.
1) When $B_s = \frac{D}{\alpha_{j+1}}$, we have:

$$g_j\left(\frac{D}{\alpha_{j+1}}\right) = \frac{\sum_{i=1}^{\hat{i}} -\lambda (-c_l \alpha_i + c_s)^\gamma \left(\frac{D}{\alpha_{j+1}}\right)^{\gamma-\beta} \gamma w(p_i)}{\sum_{i=\hat{i}+1}^{j} (c_l \alpha_i - c_s)^\beta w(p_i) \beta} + 1$$

$$- \frac{c_s \sum_{i=j+1}^{I} (c_l \alpha_{j+1} - c_s)^{\beta-1} w(p_i)}{\sum_{i=\hat{i}+1}^{j} (c_l \alpha_i - c_s)^\beta w(p_i)}. \quad (29)$$

We can obtain

$$g_j\left(\frac{D}{\alpha_{j+1}}\right) > 0 \Leftrightarrow D < H_j. \quad (30)$$

2) When $B_s = \frac{D}{\alpha_j}$, we have:

$$g_j\left(\frac{D}{\alpha_j}\right) = \frac{\sum_{i=1}^{\hat{i}} -\lambda (-c_l \alpha_i + c_s)^\gamma \left(\frac{D}{\alpha_j}\right)^{\gamma-\beta} \gamma w(p_i)}{\sum_{i=\hat{i}+1}^{j} (c_l \alpha_i - c_s)^\beta w(p_i) \beta} + 1$$

$$- \frac{c_s \sum_{i=j+1}^{I} (c_l \alpha_j - c_s)^{\beta-1} w(p_i)}{\sum_{i=\hat{i}+1}^{j} (c_l \alpha_i - c_s)^\beta w(p_i)}. \quad (31)$$

We can obtain

$$g_j\left(\frac{D}{\alpha_j}\right) > 0 \Leftrightarrow D < M_j. \quad (32)$$

We can see that $g_j(B_s)$ and $U'(B_s)$ in (28) have the same sign within the interval $\left[\frac{D}{\alpha_{j+1}}, \frac{D}{\alpha_j}\right]$. From (30), we have that $U'\left(\frac{D}{\alpha_{j+1}}\right) \geq 0$ when $D \geq H_j$ and $U'\left(\frac{D}{\alpha_{j+1}}\right) < 0$ when $D < H_j$. From (32), we have that $U'\left(\frac{D}{\alpha_j}\right) \geq 0$ when $D \geq M_j$ and $U'\left(\frac{D}{\alpha_j}\right) < 0$ when $D < M_j$. Thus $U'(B_s)$ can be either negative within the entire interval $\left[\frac{D}{\alpha_{j+1}}, \frac{D}{\alpha_j}\right]$, or positive within the entire interval, or first positive and then negative within that interval based on the value of demand parameters H_j and M_j.

To sum up, the optimal solution $B_{s,j}^*$ in each sub-interval $B_s \in \left[\frac{D}{\alpha_{j+1}}, \frac{D}{\alpha_j}\right]$, $j = \hat{i}+1, ..., I-1$ depends on the value of demand parameters H_j and M_j as in (25). ∎

Then we are going to study the cases at the boundaries of the interval $\left[\frac{D}{\alpha_I}, \frac{D c_l}{c_s}\right]$. The case of left boundary ($B_s = \frac{D}{\alpha_I}$) is included in Proposition 1. When $B_s > \frac{D}{\alpha_{\hat{i}+1}}$, we can show the utility $U(B_s)$ in (24) is decreasing in B_s, hence the optimal $B_s^* \leq \frac{D}{\alpha_{\hat{i}+1}}$.

We then study the relation between the adjacent sub-intervals. Since (i) $U(B_s)$ is continuous, (ii) $g_j(B_s) > g_{j-1}(B_s)$ for all j, and (iii) $g_j(B_s)$ is decreasing in B_s for all j, we know in $\left[\frac{D}{\alpha_I}, \frac{D c_l}{c_s}\right]$,

$$B_s^* = \begin{cases} \dfrac{D}{\alpha_j}, & \text{if } g_j\left(\frac{D}{\alpha_j}\right) \geq 0 \text{ and } g_{j-1}\left(\frac{D}{\alpha_j}\right) \leq 0, \\ g_j^{-1}(0), & \text{if } g_j\left(\frac{D}{\alpha_j}\right) < 0 \text{ and } g_j\left(\frac{D}{\alpha_{j+1}}\right) > 0. \end{cases} \quad (33)$$

Based on (30), (32) and (33), we can have the following summary.

$$B_s^* = \begin{cases} \dfrac{D}{\alpha_j}, & \text{if } H_j \le D \le M_{j+1}, \\ g_j^{-1}\left(0\right), & \text{if } M_j < D < H_j, \end{cases} \quad (34)$$

where $j = \hat{i}, ..., I-1$.

Case III: $B_s \in \left(\dfrac{Dc_l}{c_s}, \infty\right)$. In this case, $Dc_l - B_s c_s < 0$. From (7) and (11), we know

$$R\left(B_s, B_l^*, \alpha\right) - R_p = Dc_l - B_s c_s - \max\{D - B_s\alpha, 0\} < 0, \quad (35)$$

which means the total cost of sensing $B_s c_s$ will be larger than the cost of only using spectrum leasing Dc_l. However, the amount of revenue $D\pi$ from sensing or leasing is the same, since the total demand is limited. Hence it is impossible to choose the optimal B_s^* in this range to maximize the utility.

By summarizing the analysis of the above three cases, we obtain Table II.

B. Proof of Corollary 1

From (26), we obtain

$$h_\lambda\left(\lambda\right) \triangleq \frac{\partial U'\left(B_s\right)}{\partial \lambda} = \sum_{i=1}^{\hat{i}} -\gamma w(p_i)\left(c_s - c_l\alpha_i\right)^\gamma B_s^{\gamma-1} < 0, \quad (36)$$

and

$$h_\gamma\left(\gamma\right) \triangleq \frac{\partial U'\left(B_s\right)}{\partial \gamma} = \sum_{i=1}^{\hat{i}} -\lambda w(p_i)\left(c_s - c_l\alpha_i\right)^\gamma B_s^{\gamma-1}$$
$$+ \sum_{i=1}^{\hat{i}} -\lambda w(p_i)\gamma \ln\left(c_s - c_l\alpha_i\right)\left(c_s - c_l\alpha_i\right)^\gamma$$
$$- B_s^{\gamma-1} \sum_{i=1}^{\hat{i}} \lambda w(p_i)\gamma \ln B_s\left(c_s - c_l\alpha_i\right)^\gamma B_s^{\gamma-1} < 0. \quad (37)$$

If $\lambda_1 > \lambda_2$, then $h_\lambda\left(\lambda_1\right) < h_\lambda\left(\lambda_2\right)$ for every B_s, which means $U'\left(B_s\right)$ with $\lambda = \lambda_1$ is less than $U'\left(B_s\right)$ with $\lambda = \lambda_2$ for every B_s, and $U'\left(B_s\right)$ with $\lambda = \lambda_1$ will become zero with a smaller B_s. Hence B_s^* decreases in λ.

If $\gamma_1 > \gamma_2$, then $h_\gamma\left(\gamma_1\right) < h_\gamma\left(\gamma_2\right)$ for every B_s, which means $U'\left(B_s\right)$ with $\gamma = \gamma_1$ is less than $U'\left(B_s\right)$ with $\gamma = \gamma_2$ for every B_s, and $U'\left(B_s\right)$ with $\gamma = \gamma_1$ will be zero with a smaller B_s. Hence B_s^* decreases in γ when $D > M_I$.

C. Proof of Corollary 2

From (21), we obtain

$$h_\beta\left(\beta\right) \triangleq \frac{\partial U'(B_s)}{\partial \beta} = \sum_{i=\hat{i}+1}^{I} w(p_i)\left(c_l\alpha_i - c_s\right)^\beta B_s^{\beta-1}$$
$$- \sum_{i=\hat{i}+1}^{I} \lambda w(p_i)\beta \ln\left(c_l\alpha_i - c_s\right)\left(c_l\alpha_i - c_s\right)^\beta$$
$$- B_s^{\beta-1} \sum_{i=\hat{i}+1}^{I} \lambda w(p_i)\beta \ln B_s\left(c_l\alpha_i - c_s\right)^\beta B_s^{\beta-1} < 0. \quad (38)$$

If $\beta_1 > \beta_2$, then $h_\beta\left(\beta_1\right) < h_\beta\left(\beta_2\right)$ for every B_s, which means $U'\left(B_s\right)$ with $\beta = \beta_1$ is less than $U'\left(B_s\right)$ with $\beta = \beta_2$ for every B_s, and $U'\left(B_s\right)$ with $\beta = \beta_1$ will be zero with a smaller B_s. Hence B_s^* decreases in β.

D. Proof of Corollary 3

From (26), we obtain

$$h_{c_s}\left(c_s\right) \triangleq \frac{\partial U'\left(B_s\right)}{\partial c_s} = \sum_{i=1}^{\hat{i}} -\lambda\gamma^2 w(p_i)\left(c_s - c_l\alpha_i\right)^{\gamma-1} B_s^{\gamma-1}$$
$$+ c_s \sum_{i=j+1}^{I} B_s\beta\left(\beta-1\right) w(p_i)\left(Dc_l - B_s c_s\right)^{\beta-2}$$
$$- \sum_{i=j+1}^{I} \beta\left(Dc_l - B_s c_s\right)^{\beta-1} w(p_i)$$
$$- \sum_{i=\hat{i}+1}^{j} \beta^2 w(p_i)\left(c_l\alpha_i - c_s\right)^{\beta-1} B_s^{\beta-1} < 0. \quad (39)$$

If $c_s^1 > c_s^2$, then $h_{c_s}\left(c_s^1\right) < h_{c_s}\left(c_s^2\right)$ for every B_s, which means $U'\left(B_s\right)$ with $c_s = c_s^1$ is less than $U'\left(B_s\right)$ with $c_s = c_s^2$ for every B_s, and $U'\left(B_s\right)$ with $c_s = c_s^1$ will be zero with a smaller B_s. Hence B_s^* decreases in c_s.

E. The EUT Benchmark in Section IV

For comparison, we also consider the operator's optimal sensing and leasing decisions under the EUT model. As mentioned in Section III, EUT model is a special case of the PT model with $\beta = 1$, $\gamma = 1$, $\lambda = 1$, and $\mu = 1$. Under the EUT model, we can obtain the solution of problem (10) analytically.

Theorem 4. *The optimal sensing decision B_s^* for problem (10) and the optimal leasing decision B_l^* for problem (5) under EUT are summarized in Table V.*

Proof: In the proof, we divide the feasible range of B_s into two intervals, $\left[0, \dfrac{D}{\alpha_1}\right]$, and $\left[\dfrac{D}{\alpha_1}, \infty\right)$.

1) Case I: $B_s \le \dfrac{D}{\alpha_1}$. We first compute the optimal decision B_s^* in this interval. In this case, $B_s\alpha$ is not always larger than D, thus by (9), we can write the expectation of revenue $R\left(B_s, B_l^*, \alpha\right)$ with respect to α. In each sub-interval $0 \le B_s \le \dfrac{D}{\alpha_I}$[18] and $\dfrac{D}{\alpha_{j+1}} \le B_s \le \alpha_j$, $j = 1, ..., I-1$, we can write

$$U\left(B_s\right) = \mathbb{E}_\alpha\left[R\left(B_s, B_l^*, \alpha\right)\right]$$
$$= \left(\pi D - B_s c_s\right)\sum_{i=j+1}^{I} p_i + \sum_{i=1}^{j}\left[\left(\pi - c_l\right)D - B_s\left(c_s - c_l\alpha_i\right)\right]p_i$$
$$= \pi D - \sum_{i=1}^{j} p_i Dc_l + \left[\left(\sum_{i=1}^{j}\alpha_i p_i\right)c_l - c_s\right]B_s. \quad (40)$$

[18]In the case $0 \le B_s \le \dfrac{D}{\alpha_I}$, the utility function $U\left(B_s\right)$ is equivalent to $U\left(B_s\right)$ in (40) with $j = I$.

TABLE V
OPTIMAL SENSING DECISION AND LEASING DECISION UNDER EUT

Condition	Optimal Sensing Decision B_s^*	Optimal Leasing Decision B_l^*
$\frac{c_l}{c_s} \leq \left(\sum\limits_{i=1}^{I} p_i\alpha_i\right)^{-1}$	$B_s^* = 0$	$B_l^* = D$
$\left(\sum\limits_{i=1}^{j+1} p_i\alpha_i\right)^{-1} < \frac{c_l}{c_s} < \left(\sum\limits_{i=1}^{j} p_i\alpha_i\right)^{-1}$ for $j=1,...,I-1$	$B_s^* = \min\{\frac{D}{\alpha_{j+1}}, \frac{Dc_l}{c_s}\}$	$B_l^* = \max\{0, D - \alpha\min\{\frac{D}{\alpha_{j+1}}, \frac{Dc_l}{c_s}\}\}$
$\frac{c_l}{c_s} \geq (\alpha_1 p_1)^{-1}$	$B_s^* = \frac{D}{\alpha_1}$	$B_l^* = D - \alpha\frac{D}{\alpha_1}$

From (40), we know that $U(B_s)$ is continuous and piece-wise linear in B_s. Since $\sum\limits_{i=1}^{j} \alpha_i p_i c_l$ in (41) is increasing in j, we know that there is at most one local maximum point. Hence, the optimal B_s^* is either at the local maximum point or the boundaries, depending on the value of $\frac{c_l}{c_s}$,

$$B_s^* = \begin{cases} 0, & \text{if } \frac{c_l}{c_s} \leq \left(\sum\limits_{i=1}^{I} \alpha_i p_i\right)^{-1}. \\ \frac{D}{\alpha_j}, & \text{if } \left(\sum\limits_{i=1}^{j+1} \alpha_i p_i\right)^{-1} < \frac{c_l}{c_s} < \left(\sum\limits_{i=1}^{j} \alpha_i p_i\right)^{-1}, \ j=1,2,...,I-1, \\ \frac{D}{\alpha_1}, & \text{if } \frac{c_l}{c_s} \geq (\alpha_1 p_1)^{-1}. \end{cases}$$
(41)

From the analysis of Case III in Appendix A, we know that the optimal $B_s^* \in \left[0, \frac{Dc_l}{c_s}\right]$. By comparing the value of $\frac{Dc_l}{c_s}$ with the optimal B_s^* in (40), we obtain the results in the first two rows of Table V.

3) Case II: $B_s \in \left[\frac{D}{\alpha_1}, \infty\right)$.
In this case, $B_s\alpha \geq D$. From (9), we know

$$U(B_s) = \mathbb{E}[R(B_s, B_l^*, \alpha)] = \pi D - B_s c_s. \quad (42)$$

Since $R(B_s)$ is decreasing in B_s in this case, the optimal sensing decision $B_s^* = \frac{D}{\alpha_1}$, and the corresponding utility $U(B_s^*) = \pi D - \frac{D}{\alpha_1} c_s$

Since $U(B_s)$ is continuous, we combine the optimal utilities from Case I and Cases II, and obtain the optimal B_s^* with different values of $\frac{c_l}{c_s}$ as in Table V. ■

The results in Table V also depend on the cost ratio $\frac{c_l}{c_s}$. When $\frac{c_l}{c_s} \leq \left(\sum_{i=1}^{I} p_i\alpha_i\right)^{-1}$, the leasing is cheap enough so that the operator will choose to lease only ($B_s^* = 0$). For the case $\frac{c_l}{c_s} \geq (p_1\alpha_1)^{-1}$ (hence leasing is significantly more expensive), we have $B_s^* = \frac{D}{\alpha_1}$. The threshold value $\left(\sum_{i=1}^{j} p_i\alpha_i\right)^{-1}$ is based on the distribution of α, as the expected "effective cost" of getting one unit of idle spectrum through sensing is $c_s\left(\sum_{i=1}^{j} p_i\alpha_i\right)^{-1}$.

F. Proof of Theorem 2

From (12), when $B_s > D$, $U(B_s)$ is decreasing in B_s, so $B_s^* \in [0, D]$. Hence, we obtain

$$U(B_s) = -\lambda w(p_1)(B_s c_s)^\beta + (c_l - c_s)^\beta B_s^\beta w(p_2)$$
$$= \left[w(p_2)(c_l - c_s)^\beta - \lambda w(p_1) c_s{}^\beta\right] B_s^\beta. \quad (43)$$

From (43), we find that $U(B_s)$ is a monotonic function of B_s. Hence, we can find the optimal sensing decision

$$B_s^* = \begin{cases} 0, & \text{if } w(p_2)(c_l - c_s)^\beta < \lambda w(p_1) c_s{}^\beta, \\ D, & \text{if } w(p_2)(c_l - c_s)^\beta \geq \lambda w(p_1) c_s{}^\beta. \end{cases} \quad (44)$$

G. Proof of Theorem 3

From (13) and (14), when $B_s > D$, both $U_{RPH}(B_s)$ and $U_{RPL}(B_s)$ are decreasing in B_s, so $B_s^* \in [0, D]$. We prove Theorem 3 by capturing the unimodal structure of (13) and (14). For a unimodal problem, the optimal point is either at the unique local maximum point or the boundaries. We first compute the first order derivatives of U_{RPH} and U_{RPL} with respect to B_s:

$$\frac{\partial U_{RPH}(B_s)}{\partial B_s} = -\lambda c_s w(p_1)\beta[B_s c_s + D(c_l - c_s)]^{\beta-1} + \lambda w(p_2)\beta(c_l - c_s)^\beta[(D - B_s)]^{\beta-1},$$
(45)

and

$$\frac{\partial U_{RPL}(B_s)}{\partial B_s} = -c_s\beta(-B_s c_s + Dc_s)^{\beta-1}w(p_1) + \beta(c_l - c_s)[B_s(c_l - c_s) + Dc_s]^{\beta-1}w(p_2). \quad (46)$$

Since the second order derivatives $\frac{\partial^2 U_{RPH}(B_s)}{\partial B_s^2} > 0$ and $\frac{\partial^2 U_{RPL}(B_s)}{\partial B_s^2} < 0$, the function $\frac{\partial U_{RPH}}{\partial B_s}$ is a strictly increasing function of B_s, and the function $\frac{\partial U_{RPL}(B_s)}{\partial B_s}$ is a strictly decreasing function of B_s, which means $\frac{\partial U_{RPH}(B_s)}{\partial B_s}$ and $\frac{\partial U_{RPL}(B_s)}{\partial B_s}$ will only be zero at most once, thus at most one local maximum point for both $U_{RPH}(B_s)$ and $U_{RPL}(B_s)$.

We then consider the two boundary points (a) $B_s = 0 + \epsilon$ and (b) $B_s = D - \epsilon$, with ϵ being a small positive number approaching zero (i.e., $\epsilon \to 0$), to see if the optimal point is at the local maximum point or at the boundaries.

(a) When $B_s = 0 + \epsilon$, we have:

$$\lim_{\epsilon \to 0} U'_{RPH}(\epsilon) = \beta\lambda[D(c_l - c_s)]^{\beta-1}[w(p_2)(c_l - c_s) - w(p_1)c_s], \quad (47)$$

and

$$\lim_{\epsilon \to 0} U'_{RPL}(\epsilon) = \beta Dc_s^{\beta-1}[-w(p_1)c_s + (c_l - c_s)w(p_2)]. \quad (48)$$

(b) When $B_s = D - \epsilon$, we have:

$$\lim_{\epsilon \to 0} U'_{RPH}(D - \epsilon) = \infty, \quad (49)$$

and

$$\lim_{\epsilon \to 0} U'_{RPL} (D - \epsilon) = -\infty. \qquad (50)$$

We can obtain

$$\lim_{\epsilon \to 0} U'_{RPH} (\epsilon) < 0 \Leftrightarrow - w(p_1) c_s + (c_l - c_s) w(p_2) < 0$$

$$\Leftrightarrow \lim_{\epsilon \to 0} U_{RPL} (\epsilon) < 0. \qquad (51)$$

Since $U'_{RPH} (\epsilon)$ and $U'_{RPL} (\epsilon)$ have the same sign from (47) and (48), either $U'_{RPH} (B_s)$ is first negative then positive and $U'_{RPL} (B_s)$ is all negative within the range $(0, D)$, or $U'_{RPH} (B_s)$ is all positive and $U'_{RPL} (B_s)$ is first positive then negative within the range $(0, D)$.

Since $U(B_s)$ is continuous in $B_s \in [0, D]$, the optimal solution B_s^* under the two reference points depends on the value of c_l and c_s as in Table IV.
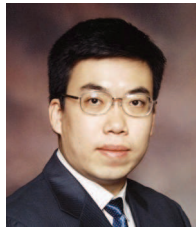
Jianwei Huang (F'16) is an Associate Professor and Director of the Network Communications and Economics Lab (ncel.ie.cuhk.edu.hk), in the Department of Information Engineering at the Chinese University of Hong Kong. He received the Ph.D. degree from Northwestern University in 2005. He is the co-recipient of 8 Best Paper Awards, including IEEE Marconi Prize Paper Award in Wireless Communications in 2011. He has co-authored five books: *Wireless Network Pricing*, *Monotonic Optimization in Communication and Networking Systems*, *Cognitive Mobile Virtual Network Operator Games*, *Social Cognitive Radio Networks*, and *Economics of Database-Assisted Spectrum Sharing*. He has served as an Associate Editor of IEEE Transactions on Cognitive Communications and Networking, IEEE Transactions on Wireless Communications, and IEEE Journal on Selected Areas in Communications - Cognitive Radio Series. He is the Vice Chair of IEEE ComSoc Cognitive Network Technical Committee and the Past Chair of IEEE ComSoc Multimedia Communications Technical Committee. He is a Fellow of the IEEE and a Distinguished Lecturer of IEEE Communications Society.

Junlin Yu (S'14) is working towards his Ph.D. degree in the Department of Information Engineering at the Chinese University of Hong Kong. His research interests include behavioral economical studies in wireless communication networks, and optimization in mobile data trading. He is a student member of IEEE.

Man Hon Cheung received the B.Eng. and M.Phil. degrees in Information Engineering from the Chinese University of Hong Kong (CUHK) in 2005 and 2007, respectively, and the Ph.D. degree in Electrical and Computer Engineering from the University of British Columbia (UBC) in 2012. Currently, he is a postdoctoral fellow in the Department of Information Engineering in CUHK. He received the IEEE Student Travel Grant for attending *IEEE ICC 2009*. He was awarded the Graduate Student International Research Mobility Award by UBC, and the Global Scholarship Programme for Research Excellence by CUHK. He serves as a Technical Program Committee member in *IEEE ICC*, *Globecom*, and *WCNC*. His research interests include the design and analysis of wireless network protocols using optimization theory, game theory, and dynamic programming, with current focus on mobile data offloading, mobile crowd sensing, and network economics.